

Electronic Supplementary Information

Vapor-phase hydrothermal transformation of nanosheet array structure Ni(OH)₂ into ultrathin Ni₃S₂ nanosheets on nickel foam for high-efficiency overall water splitting

Guoqiang Liu^{a,b,†}, Zhongti Sun^{c,†}, Xian Zhang,^{a,b} Haojie Wang^{a,b}, Guozhong Wang^a,
Xiaojun Wu^c, Haimin Zhang^{*a}, Huijun Zhao^{a,d}

^a Key Laboratory of Materials Physics, Centre for Environmental and Energy Nanomaterials, Anhui Key Laboratory of Nanomaterials and Nanotechnology, CAS Center for Excellence in Nanoscience, Institute of Solid State Physics, Chinese Academy of Sciences, Hefei 230031, China.

^b University of Science and Technology of China, Hefei 230026, China.

^c CAS Key Laboratory of Materials for Energy Conversion and Department of Material Science and Engineering, University of Science and Technology of China, Hefei, Anhui 230026, People's Republic of China

^d Centre for Clean Environment and Energy, Griffith University, Gold Coast Campus, QLD 4222, Australia.

* Corresponding author: Fax: +86 (0)551 65591434; Tel: +86 (0)551 65591973;
zhanghm@issp.ac.cn

Table S1 Comparison of OER property of Ni₃S₂/NF-2 with other nonnoble-metal electrocatalysts in 1.0 M KOH electrolyte.

Catalyst	J (mA cm ⁻²)	Overpotential (mV)	Ref.
Co ₃ O ₄ /Co(OH) ₂ -8	10	373	1
Ni(OH) ₂ /Ni ₃ S ₂ -12	20	300	2
NiCo ₂ O ₄ /Ni ₃ S ₂ /NF	40	360	3
MnCo ₂ S ₄	50	325	4
Fe(TCNQ) ₂	50	353	5
Ni(OH) ₂ -TCNQ	100	354	6
Ni _{2.3%} -CoS ₂ /CC	100	370	7
Co-P	100	413	8
Co-S/Ti	100	430	9
Ni ₃ S ₂ /NF-2	100	425	This work

Table S2 The adsorption energy of N₂H₄ and H₂O molecule (ΔE , in the unit of eV), the O-H bond length of H₂O (D_{O-H} , in the unit of Å), the N-N and N-H of N₂H₄ (D_{N-N} and D_{N-H} , in the unit of Å), the H-O-H bond angle of H₂O ($\angle H-O-H$, in the unit of °), the H-N-N and H-N-H bond angle of N₂H₄ ($\angle H-N-N$ and $\angle H-N-H$, in the unit of °), the charge transfer through bader analysis, negative value indicates electron accumulations.

	ΔE	D_{O-H}	D_{N-N}	D_{N-H}	$\angle H-O-H$	$\angle H-N-N$	$\angle H-N-H$	Charge
H ₂ O-1	-0.82	0.985	-	-	105.597	-	-	-0.0511

H ₂ O -2	-0.17	0.977	-	-	104.964	-	-	-0.0166
N ₂ H ₄ -1	-1.35	-	1.459	1.031	-	111.943	108.814	-0.1464
N ₂ H ₄ -2	-1.41	-	1.450	1.030	-	112.625	107.777	-0.1216
H ₂ O-mole	-	0.972	-	-	104.533	-	-	-
N ₂ H ₄ -mole	-	-	1.488	1.029	-	103.871	102.403	-

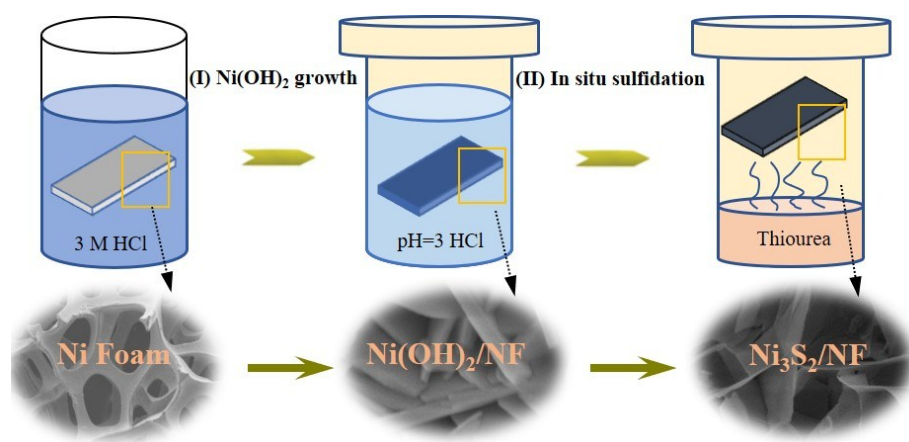


Fig. S1 Schematic illustration of the fabrication processes of Ni₃S₂/NF.

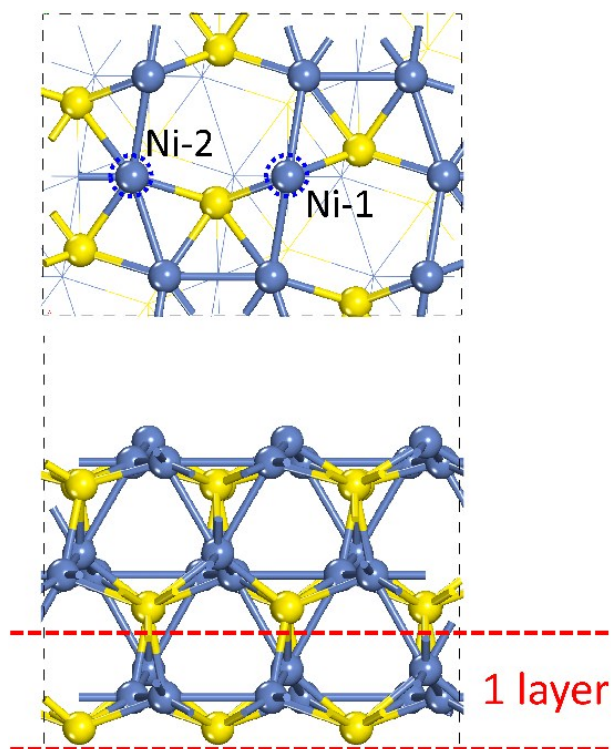


Fig. S2 The top (up) and side (down) $\text{Ni}_3\text{S}_2(110)$ surface model with three atomic layer, one atomic layer with two red dashed line was composed of three Ni_3S_2 unit, Ni and S atom in light blue and yellow, respectively. The dashed blue circle indicates low and high coordinate Ni atoms, named as Ni-1 and Ni-2, respectively.

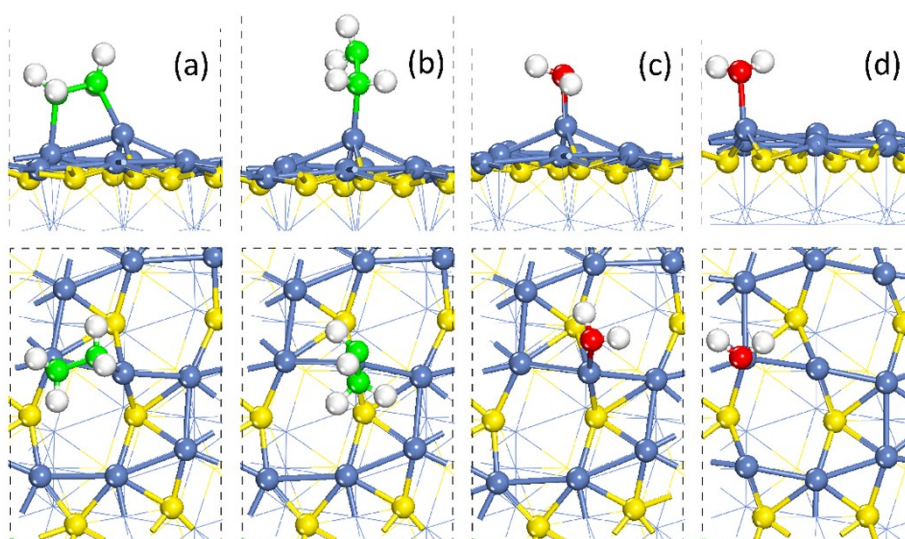


Fig. S3 The possible adsorption configurations of N_2H_4 and H_2O molecule with side (up) and top (down) view, named as (a) N_2H_4 -1, (b) N_2H_4 -2, (c) H_2O -1, (d) H_2O -2. Ni, S, O, N, and H in light blue, yellow, red, green and white, respectively.

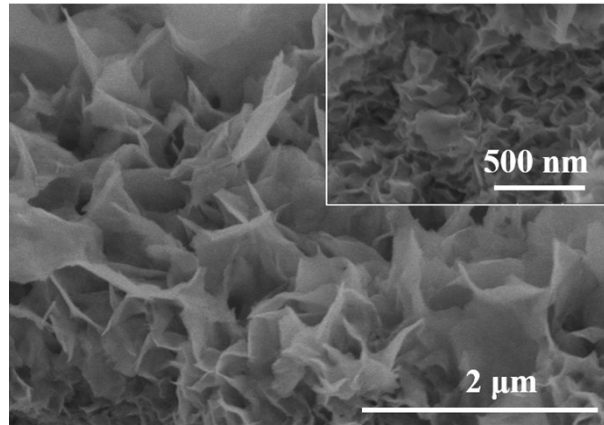


Fig. S4 SEM images of $\text{Ni}_3\text{S}_2/\text{NF-3}$.

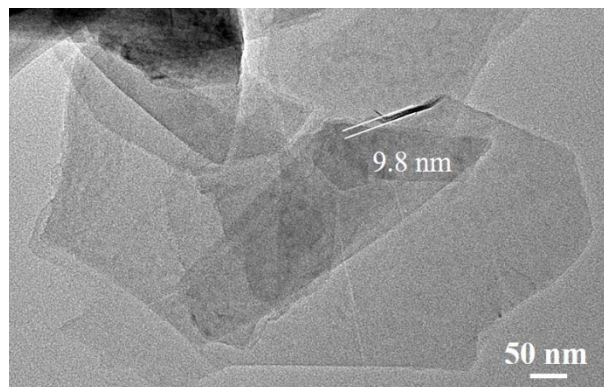


Fig. S5 TEM image of $\text{Ni}_3\text{S}_2/\text{NF-2}$ with overlapped nanosheet.

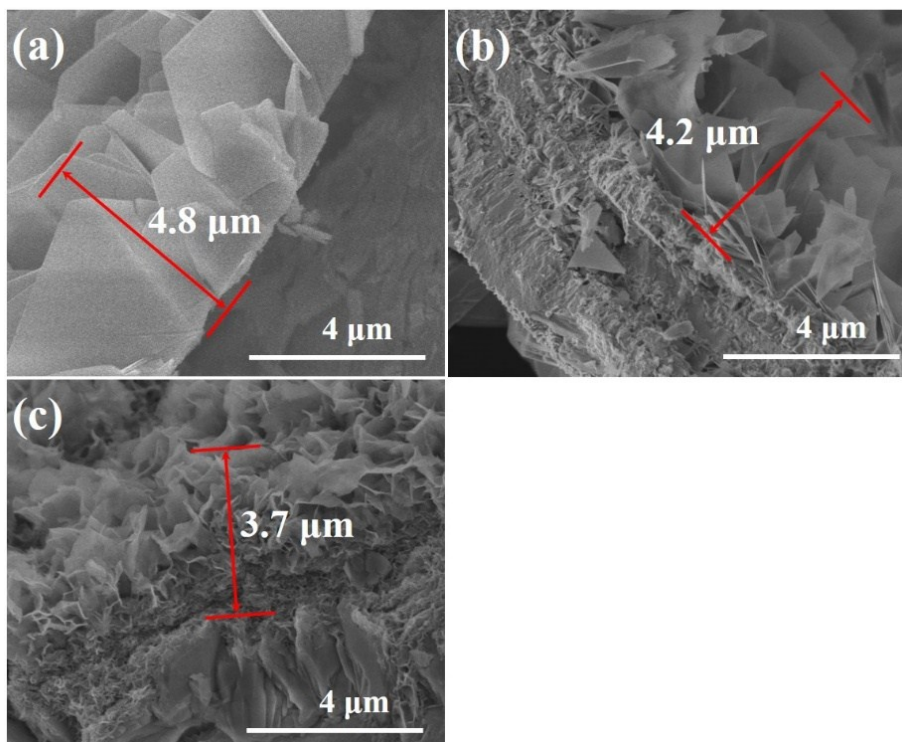


Fig. S6 Cross-sectional SEM images of (a) Ni₃S₂/NF-1, (b) Ni₃S₂/NF-2 and (c) Ni₃S₂/NF-3.

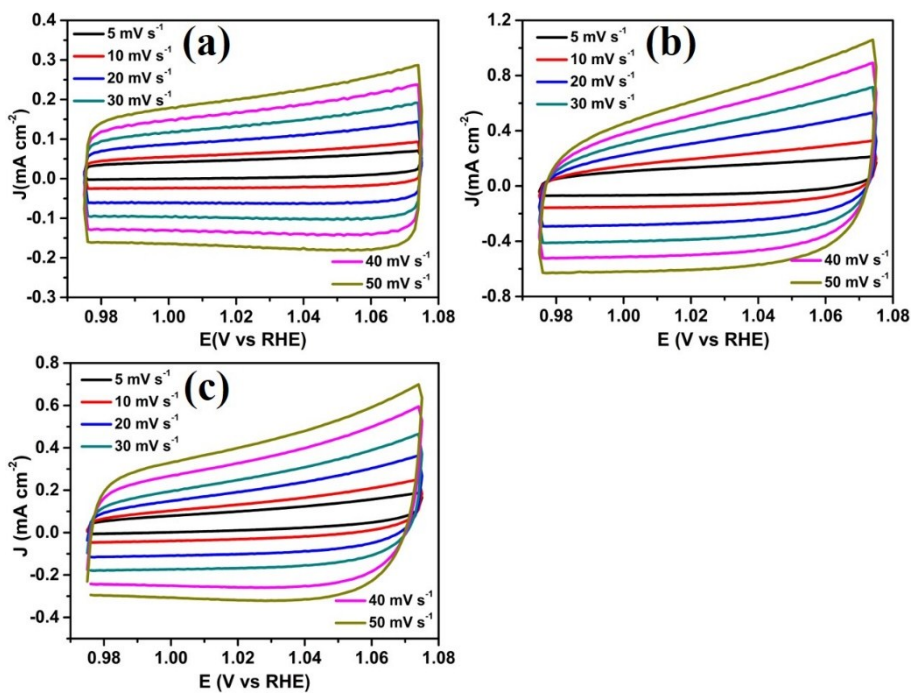


Fig. S7 Cyclic voltammogram measurements of (a) Ni₃S₂/NF-1, (b) Ni₃S₂/NF-2 and (c) Ni₃S₂/NF-3 with different scanning rates in 1.0 M KOH.

To appraise the electrochemical capacitance surface area (ECSA) of the as-prepared samples, we record the electrochemical double-layer capacitances (C_{dl}) by

CV curves in the sweeping region without faradaic process happens.¹⁰ CV measurements are swept from 0.975 to 1.075 V vs. RHE electrode with different scan rates of 5, 10, 20, 30, 40 and 50 mV s⁻¹. The electrochemical double-layer capacitive current densities are measured at 1.025 V vs. RHE and plotted as a function with scan rate to obtain electrochemical double-layer capacitance (C_{dl} , the slope of the current density vs. scan rate plots). The ECSA is proportional to their C_{dl} .¹¹

The obtained potentials in all experiment were converted into the potentials vs. RHE (reversible hydrogen electrode), according to the equation of E (vs. RHE) = E^0 (vs. Hg/HgO) + 0.098 V + 0.059pH, (0.098 V is the standard electrode potential for Hg/HgO at 25°C).¹²

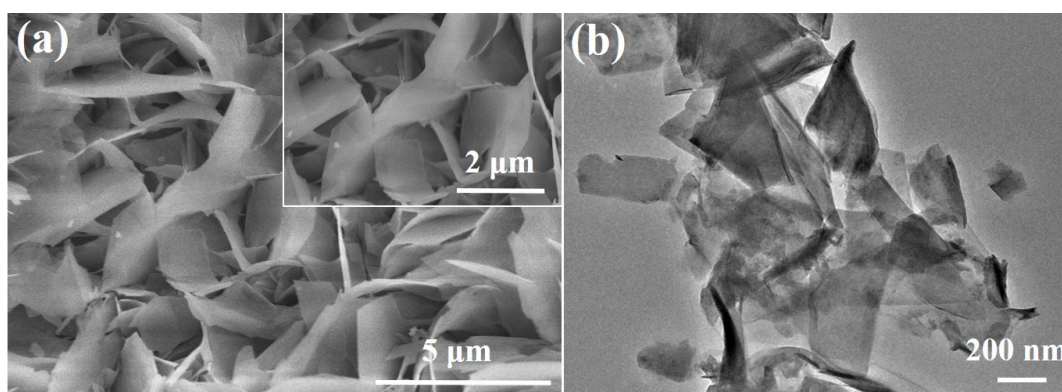


Fig. S8 (a) SEM and (b) TEM images of Ni₃S₂/NF-2 after long-term stability test of OER process.

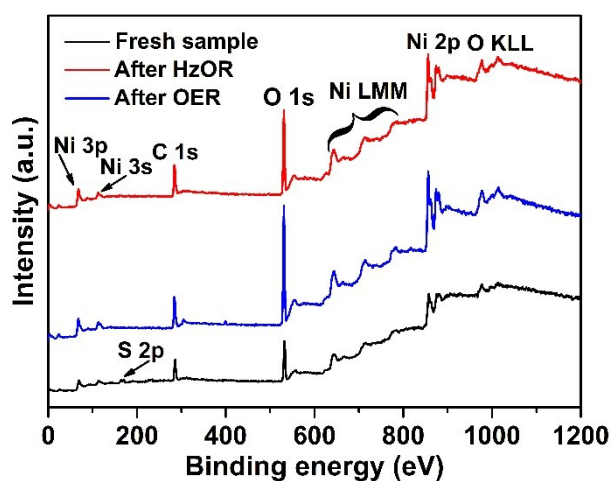


Fig. S9 Survey XPS spectra of Ni₃S₂/NF-2 before (fresh sample) and after electrocatalytic HzOR and OER process.

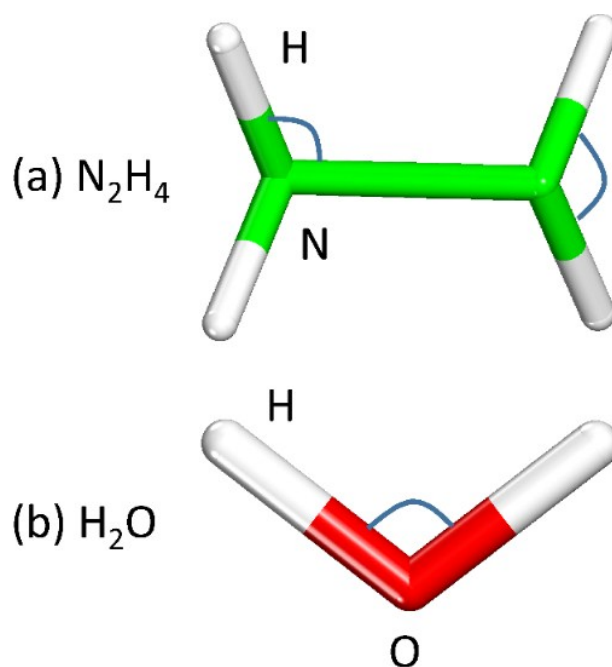


Fig. S10 The molecule model of (a) N₂H₄ and (b) H₂O, among O, N and H in red, green, white, respectively.

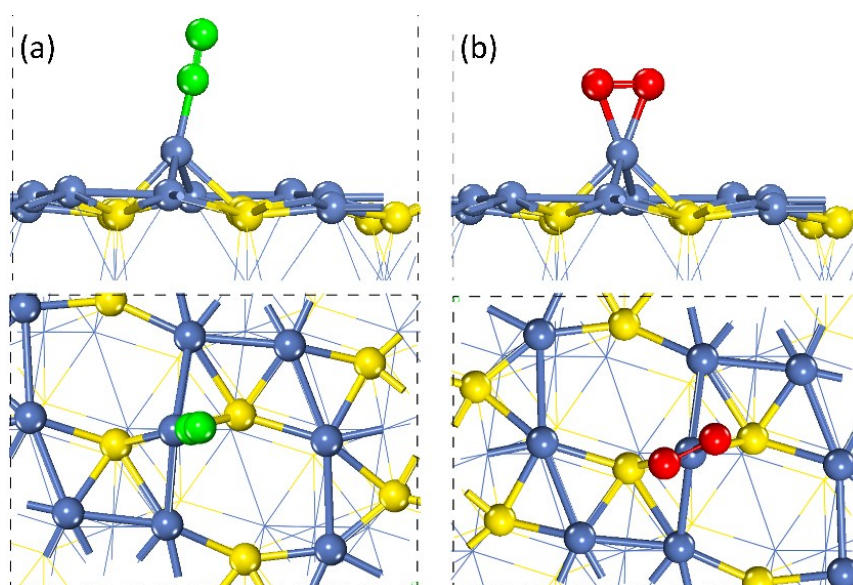


Fig. S11 The side (up) and top (down) view of adsorption configurations of (a) N₂ and

(b) O₂ molecules on the Ni₃S₂ (110) surface. Ni, S, O and N in light blue, yellow, red and green, respectively.

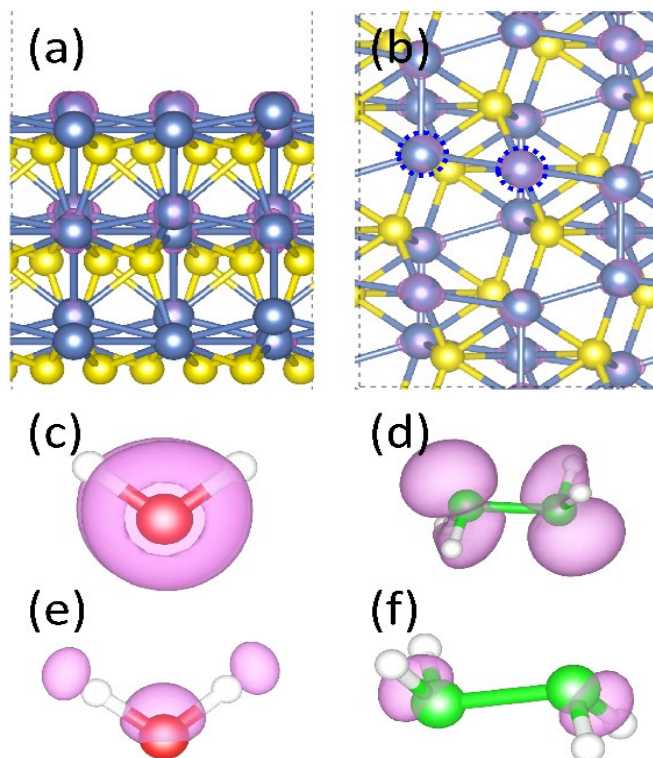


Fig. S12 The partial charge density of Ni₃S₂(110) surface around fermi level of 0.1 eV with side (a) and top (b) view, H₂O and N₂H₄ molecule with HOMO (c, d) and LUMO (e, f). The iso-surface value with pink contour is 0.01 e/bohr³. Ni, S, O, N, and H in light blue, yellow, red, green and white, respectively. The dashed blue circle indicates high and low coordinate Ni atoms.

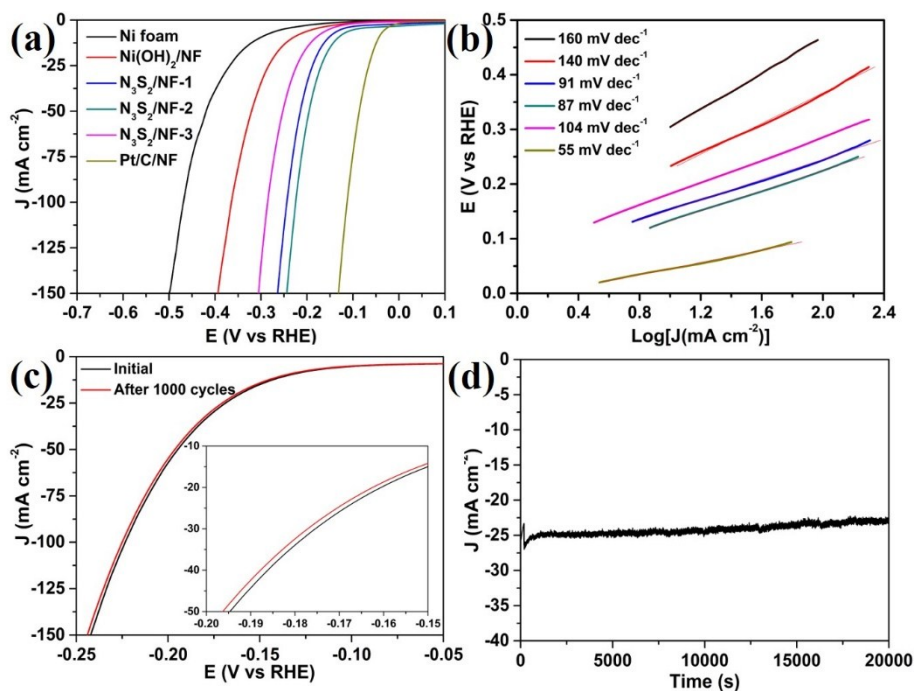


Fig. S13 (a) LSV curves with iR drop compensation and (b) the corresponding Tafel plots of NF, $\text{Ni(OH)}_2/\text{NF}$, $\text{Ni}_3\text{S}_2/\text{NF-1}$, $\text{Ni}_3\text{S}_2/\text{NF-2}$, $\text{Ni}_3\text{S}_2/\text{NF-3}$ and commercial Pt/C at a scanning rate of 5.0 mV s^{-1} . (c) and (d) HER durability tests for the $\text{Ni}_3\text{S}_2/\text{NF-2}$ electrocatalyst in 1.0 M KOH.

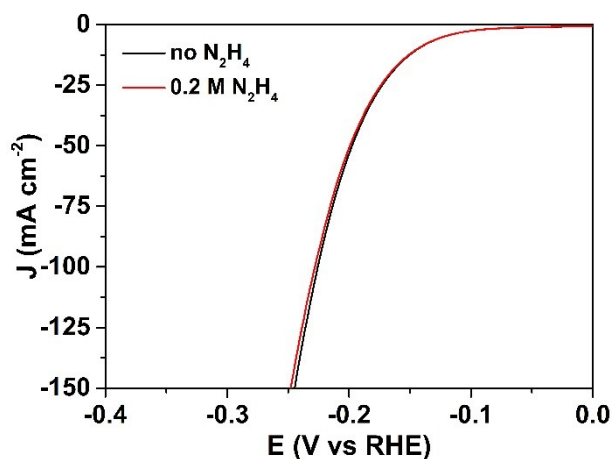


Fig. S14 LSV curves with iR drop compensation of $\text{Ni}_3\text{S}_2/\text{NF-2}$ at a scanning rate of 5.0 mV s^{-1} with (red line) and without (black line) 0.2 M hydrazine.

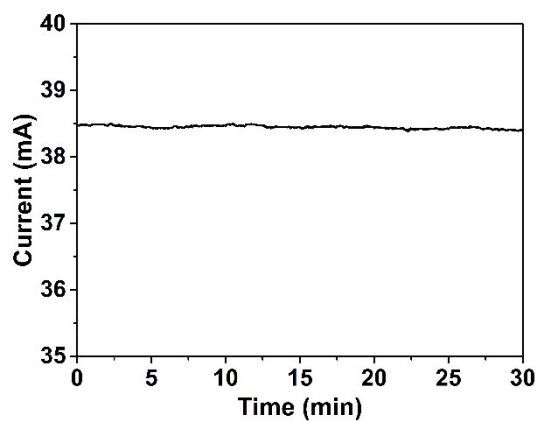


Fig. S15 The current density of $\text{Ni}_3\text{S}_2/\text{NF-2}$ catalyzed HzOR for H_2 generation with a potential of 0.75 V in two-electrode system ($\text{Ni}_3\text{S}_2/\text{NF-2}$ as both anode and cathode).

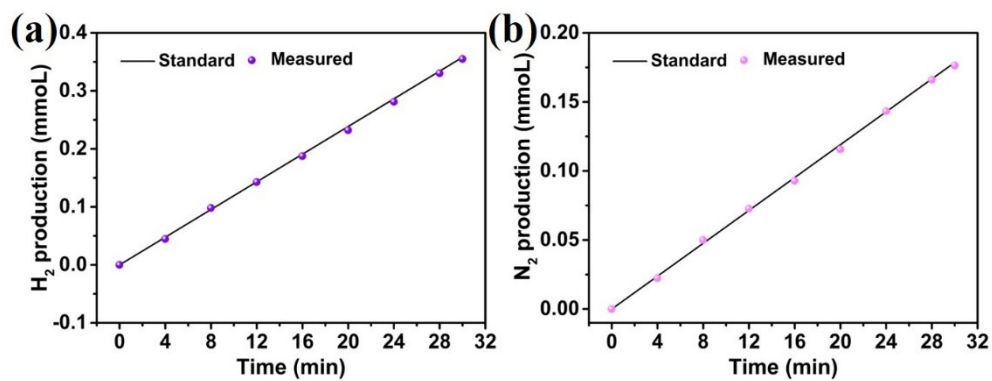


Fig. S16 The collected amount of (a) H_2 and (b) N_2 theoretically calculated and experimentally measured vs. time.

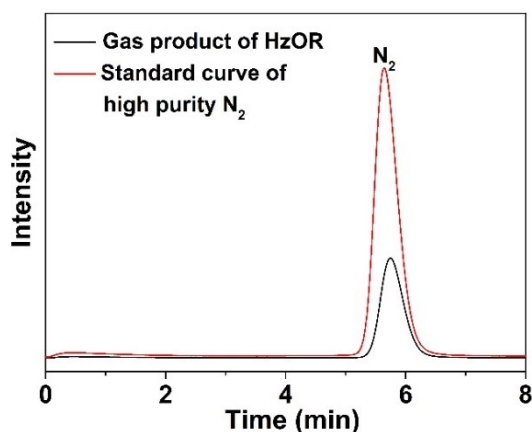


Fig. S17 Chromatograms for the HzOR production catalyzed by Ni₃S₂/NF-2 in two-electrode system with 0.2 M hydrazine in 1.0 M KOH.

The oxidation product of hydrazine was first analyzed by gas chromatography (GC, Beijing aulight Technology Co., Ltd, GC-7920).

References

- [1] X. Q. Du, H. L. Pan, Z. Yang, *New J. Chem.*, 2018, 42, 4215-4222.
- [2] X. Q. Du, Z. Yang, Y. Li, Y. Q. Gong, M. Zhao, *J. Mater. Chem. A*, 2018, 6, 6938-6946.
- [3] X. Q. Du, Q. B. Wang, Y. Li, X. S. Zhang, *Dalton T.*, 2018, 47, 10273-10280.
- [4] X. X. Guo, S. Y. Zhu, R. M. Kong, X. P. Zhang, F. L. Qu, *ACS Sustain. Chem. Eng.*, 2018, 6, 1545-1549.
- [5] X. P. Zhang, C. D. Si, X. X. Guo, R. M. Kong, F. L. Qu, *J. Mater. Chem. A*, 2017, 5, 17211-17215.
- [6] X. X. Guo, R. M. Kong, X. P. Zhang, H. T. Du, F. L. Qu, *ACS Catal.*, 2017, 8, 651-655.
- [7] W. Z. Fang, D. N. Liu, Q. Lu, X. P. Sun, A. M. Asiri, *Electrochem. Commun.*, 2016, 63, 60-64.
- [8] N. Jiang, B. You, M. L. Sheng, Y. J. Sun, *Angew. Chem., Int. Ed.*, 2015, 127, 6349-6352.
- [9] T. T. Liu, Y. H. Liang, Q. Liu, X. P. Sun, Y. Q. He, A. M. Asiri, *Electrochem. Commun.*, 2015, 60, 92-96.

- [10] C. C. L. McCrory, S. Jung, J. C. Peters, T. F. Jaramillo, *J. Am. Chem. Soc.*, 2013, 135,16977.
- [11] X. Y. Yu, Y. Feng, Y. Y. Jeon, B. Y. Guan, X.W. Lou, U. Paik, *Adv. Mater.*, 2016, 28, 9006.
- [12] J. X. Feng, S. H. Ye, H. Xu, Y. X. Tong, G. R. Li, *Adv. Mater.*, 2016, 28, 4698.